

THE VALIDATION OF MICROPHYSICS PROPERTIES SIMULATED BY A CLOUD RESOLVING MODEL USING AN IN-SITU AIRCRAFT OBSERVATION DURING A COLD WINTER EVENT

Hideaki Ohtake*, M. Murakami, N. Orikasa, A. Saito and A. Hashimoto.

Meteorological Research Institute, Tsukuba, Japan

1. Introduction

Recently, some field projects have collected comprehensive kinematic and cloud microphysical datasets over the complex topography to understand the inner structure of the cloud system and the environmental conditions around cloud system and to improve the dynamical process and the bulk microphysical parameterizations in the cloud resolving model.

Several recent studies compared the results of these models with various observational dataset. In recent studies, several comparisons and verification between the in situ aircraft observation and the results of numerical simulation has been employed (e.g., Guan et al. 2001, 2002, Colle et al. 2003; Mavromatidis and Kallos 2003; Garvert et al. 2005a, 2005b; Vaillancourt et al. 2003; Zhang et al. 2007, Luo et al., 2008a, 2008b; Milbrandt et al. 2008; Morrison et al. 2008).

In the IMPROVE-2 (The Improvement of Microphysical Parameterization through Observational Verification Experiment) project, Garvert et al. (2005b) compared airborne in situ observations of cloud microphysical parameters with the fifth-generation Pennsylvania State University-National Center for Atmospheric Research (PSU-NCAR) Mesoscale Model (MM5) simulations for a heavy precipitation event over the Oregon Cascades on 13-14 December 2001. They showed that the model produced a broader number distribution of snow particles than observed, overpredicting the number of moderate-to-large-sized snow particles and underpredicting the number of small particles observed along flight track. Mavromatidis et al. (2003) conducted a detailed comparison of the

model results with aircraft data and showed that the model-calculated water content and number concentration deviate significantly for the small size particle bin (2-47 microns) but are in good agreement for the medium size (25-800 microns) and large size (200-6400 microns) bins.

In the Mixed-Phase Arctic Cloud Experiment (MPACE) project, the model results are reasonably similar to observations in terms of the liquid microphysical properties, while the ice microphysical properties are more significantly biased (Morrison et al. 2008, Luo et al. 2008a; 2008b).

Garvert et al. 2005, Milbrandt et al. 2008 and Colle et al. 2008 examine the effect of the horizontal grid spacing of their model and they show that the 1.33-km-resolution simulation appeared to depict correctly the perturbations in vertical air motion yet it drastically overpredicted the amount of cloud liquid water (CLW). On the other hand, the 4-km resolution model better simulated the amount of CLW, but further underpredicted the amplitude of the vertical velocity forcing.

However, these mesoscale models used various microphysics schemes, as a result, various results were reported. Adequate simulation on the orographic snow clouds is needed to predict the dynamical and cloud physical properties.

The Japan Meteorology Agency/Meteorological Research Institute (JMA/MRI) has been also developed the cloud resolving nonhydrostatic model (JMA-NHM) (e.g., Saito (2006)). However, there have been few studies of the validation on the JMA-NHM based on an in-situ observation, primarily because there are few in situ observations of the cloud physical properties to evaluate model performance. Therefore, the modeling performance has not been checked enough. To assess the prediction of JMA-NHM has been desired.

The research project is now on progress to examine the cloud seeding technique enhancing the

* *Corresponding author address:* Hideaki Ohtake, Meteorological Research Institute, 1-1, Nagamine, Tsukuba, Ibaraki 305-0052, Japan. E-mail: hiohtake@mri-jma.go.jp

TABLE 1. Observed periods in March and December 2007.

| Flight | Mar-07 start(JST) | end(JST) |
|--------|-------------------|-------------------|
| No.1 | 05a | 11:59:15 14:37:47 |
| No.2 | 06a | 10:15:59 12:56:40 |
| No.3 | 07a | 12:31:22 15:47:52 |
| No.4 | 08a | 14:30:06 17:40:47 |
| No.5 | 11a | 14:14:10 17:19:37 |
| No.6 | 12a | 9:20:40 12:20:27 |
| No.7 | 12b | 14:45:32 17:27:33 |
| No.8 | 13a | 7:52:08 11:09:09 |
| No.9 | 13b | 14:12:09 17:22:41 |
| No.10 | 15a | 13:20:23 15:48:11 |

| Flight | Dec-07 start(JST) | end(JST) |
|--------|-------------------|-------------------|
| No.1 | 04a | 13:25:24 16:37:44 |
| No.2 | 05a | 10:13:18 13:29:05 |
| No.3 | 09a | 08:24:29 11:06:00 |
| No.4 | 09b | 13:29:28 15:55:43 |
| No.5 | 10a | 07:51:02 11:03:31 |
| No.6 | 14a | 13:29:09 16:43:57 |
| No.7 | 16a | 07:59:54 11:09:02 |
| No.8 | 17a | 15:07:14 17:03:24 |
| No.9 | 18a | 14:00:42 16:54:53 |
| No.10 | 19a | 07:48:06 08:50:33 |
| No.11 | 20a | 14:13:52 16:29:33 |

snowfall in Echigo Mountains (Japanese Cloud Seeding Experiment for Precipitation; JCSEPA) which is the main water reservoir for the Tokyo metropolitan area (e.g., Hashimoto et al. 2008, Kato et al., 2008, Yoshida et al. 2009). In this project, the aircraft observations on the dynamical and microphysical properties and several artificial cloud seeding experiments have been conducted in orographic snow clouds during the two winter seasons (March and December 2007).

The aim of this paper is to validate the numerical simulation of JMA-NHM using the in situ aircraft dataset and to evaluate the modeling performance on the cases of orographic snow clouds.

Section 2 gives a description of the aircraft instruments and the data processing of the aircraft dataset, which was accepted quality check. The numerical simulations using JMA-NHM are described in section 3. The results of the validation using the aircraft datasets are presented in section 4. Section 5 contains the summary and conclusions.

2. Aircraft observation

2.1 Instrumentation

During the JCSEPA campaign, a total of 21 flights with research aircraft MU-2 were conducted in

TABLE 2. Measurements of the aircraft observation.

| Instrument | variable |
|--|--|
| King LWC probe | Liquid water content(LWC) |
| Nevezorov LWC probe | LWC |
| Nevezorov TWC probe (SkyTech Research, Inc.) | Total water content(TWC) IWC(=TWC-LWC) |
| Gerber PVM-100A probe | LWC |
| PMS 2DC(25-800um) | LWC, concentration/size |
| PMS 2DP(200-6400um) | LWC, concentration/size |
| PMS FSSP-100(2-47um) | LWC, concentration/size |
| DMT CAPS (CAS:0.5-50um, CIP:25-1550um) | LWC, concentration/size |

March and December 2007. Table 1 lists the flight number, date, take off time and landing time. During 5-15 March 2007 (10 flights) and 2-20 December 2007(11 flights), the research aircraft measured a variety of basic-state parameters and microphysical data, including temperature, humidity, wind speed and direction, liquid water content (LWC), ice water content (IWC), cloud or ice particles imagery, and these concentrations.

Table 2 lists cloud microphysics instruments on the MU-2. Measurements of LWC, IWC and the number concentration of both water and ice particles has become available following some instruments. The microphysical instruments includes the Particle Measuring System (PMS) Forward Scattering Spectrometer Probe (FSSP-100; 2-47 μm ; Knollenberg 1981), PMS optical array probe-2DC (OAP-2DC; 25-800 μm), PMS OAP-2DP (200-6400 μm); Knollenberg 1981), the Droplet Measurement Technologies (DMT) cloud, aerosol, and precipitation spectrometer (CAPS; Baumgardner et al., 2001)(CAS; 0.5-50 μm), Cloud Imaging Probe (CIP; 25-1550 μm). Furthermore, PMS King Probe (King et al. 1978), a hot-wire Nevezorov liquid/total (ice + liquid) water content (LWC/TWC) probe (Korolev et al., 1998; Strapp et al. 2003) and Gerber Probe (Gerber et al., 1994) are also equipped with the MU-2.

These raw data measured by PMS King Probe LWC (KLWC) and Nevezorov LWC/TWC probe were necessary to be revised the reference based on the FSSP data. At first, we defined the concentration > 5 (#/cc) measured by FSSP for LWC as "the cloud region". Similarly, "the cloud region" for TWC was defined by the following threshold value, FSSP concentration > 5 (#/cc) or 2DC concentration > 0.1 (#/L). Nevezorov LWC/TWC was recalculated based on the raw voltage data and also revised based on the same way in KLWC data. IWC was not measured directly, so IWC was determined by subtracting LWC from TWC, that is IWC=TWC-LWC.

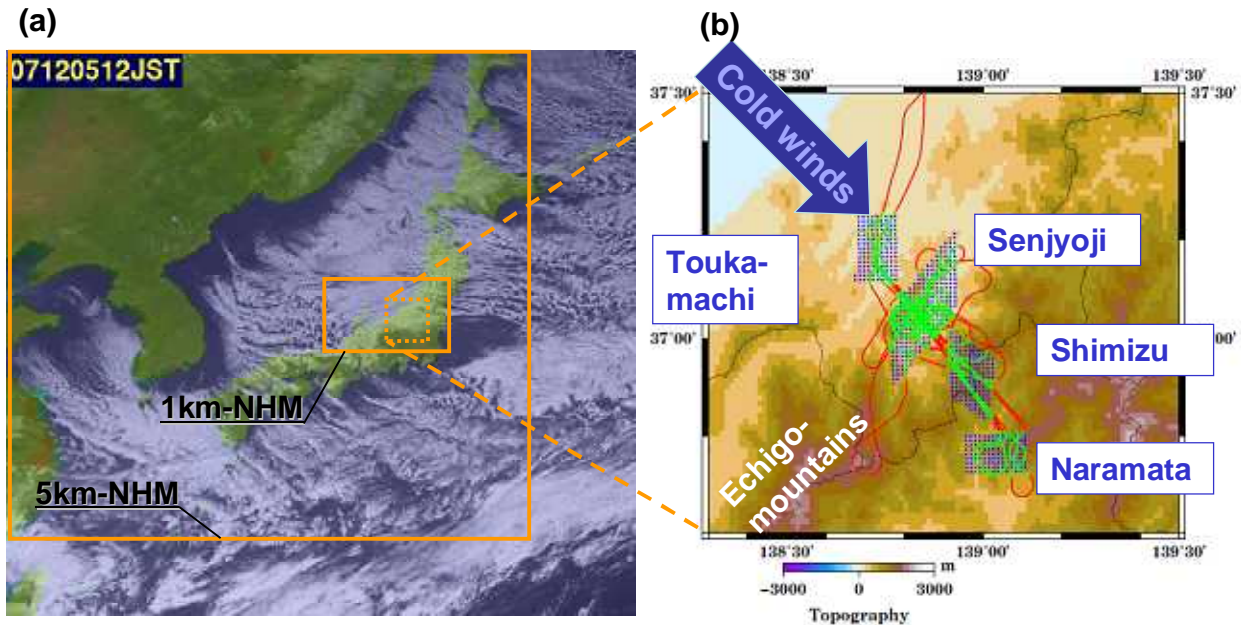


Fig. 1. (a) Geostationary Operational Environmental Satellite-9 (GOES-9) visible image at 12 LST 5 December 2007. The solid outer and inner rectangles denote the domains for 5km-NHM and 1km-NHM, respectively. (b) Close up view of the area around Echigo Mountains in the 1km-NHM domain. The red line shows the flight track on 5 December 2007. The blue dots denote the four surface observation sites (Toukamachi, Senjoji, Shimizu, Naramata). The green lines denote the flight track over the four surface observational sites.

2.2 Data processing

There is spatial and temporal mismatch between the model simulations and the aircraft observations due to the significant complexity of the real cloud fields or some problems of the model. Therefore, for evaluating the simulated variables, the simulated variables are compared with the aircraft measurements using a statistical approach. Simulated variables are averaged over the specific domains, as shown in the section 3.1, for spatial direction and averaged during 3 hours of observational periods for temporal direction to reduce the spatial and temporal mismatch. In our field projects, the cloud seeding experiments are also conducted. Therefore, the observed data during each seeding time are removed for the present validation to remove the seeding effect. After that, these observed dataset are averaged over the special observation sites for spatial and temporal directions.

3. Numerical model

3.1 Overview of snow clouds around Japan.

Figure 1a shows Geostationary Operational

Environmental Satellite-9 (GOES-9) visible image at 12 LST 5 December 2007. Hereafter, the local standard time in Japan (LST = UTC + 9 hours) will be used. This figure is the examination of the cloud fields over the sea of Japan and orographic snow clouds over the western coastal region of Echigo, center part of Japan. The orographic snow clouds in present study were observed in March and December 2007. Over the Sea of Japan, some cloud streets oriented roughly in a northwest-southwest direction also frequently appear during outbreaks of cold air, causing the locally heavy snow fall over the western coastal region of Echigo, Japan.

Figure 1b show the close up view of the region enclosed by the rectangle in Fig. 1a. The special observation sites, where several remote sensing instruments were installed, and the examination of the flight path of the MU-2 on 5 December 2007. The research aircraft flew vertically stacked horizontal flight and gathered microphysical data at a number of altitudes, thereby, providing detailed descriptions of cloud and precipitation in the orographic snow clouds.

3.2 The model

The numerical simulations were performed using

TABLE 3. Specification of 1km-NHM.

| Categories | Specification in the present model |
|---------------------------------|--|
| Basic equation | Japan Meteorological Agency NonHydrostatic Model (JMA-NHM) |
| Vertical coordinate | Terrain-following |
| Horizontal resolution | 1km |
| Horizontal grid points | 500 × 400 × 50 |
| Initial and boundary conditions | 5km horizontal resolution model (MSM) |
| water substances | cloud water, rain, cloud ice, snow and hail (Ikawa and Saito, 1991) |
| parameterization scheme | two-moment bulk parameterization (solid water) (mixing ratio and number concentration) one-moment bulk parameterization (liquid water) (mixing ratio) |

the JMA-NHM. Saito et al. (2006) have provided a comprehensive description of the model. The horizontal grid spacing is 1km (1km-NHM) and 5km (5km-NHM). Table 3 lists the specification of 1km-NHM. The model domain size of 5km-NHM and 1km-NHM is 250 × 200 × 50 and 500 × 400 × 50 in the x, y, and z, directions, respectively. The 1km-NHM is embedded into the 5 km-NHM domain. The model produced high-resolution output at every 6 minutes

for 1km-NHM for a specific region. On the microphysical process, the 1km/5km-NHM has five categories of liquid and solid water substances: cloud water, rain, cloud ice, snow, and graupel, as described in Ikawa and Saito (1991). A two-moment bulk parameterization scheme, which prognoses both the mixing ratio and number concentration, is applied to the categories of solid hydrometeor, while one-moment scheme, which prognoses only mixing ratio, are applied to those of liquid hydrometeor. Hashimoto et al. (2009) have explained the setting of the numerical simulations in detail, except for that the cloud seeding experiments were not conducted in the numerical simulations analyzed in this paper.

Figure 2a shows the concentration of both snow and ice at $z^*=1.94\text{km}$ for simulated by 5km-NHM. This figure means that this model can reproduce the synoptic-scale cloud pattern compared to the satellite image (see Fig. 1a). Figure 2b also shows the vertical accumulated of both snow and ice for simulated by 1km-NHM at the same time. The remarkably thick cloud band oriented in a west-east direction is occurred by the cloud resolving model. In the northern region of the cloud band, however, there is no cloud field though some cloud fields are found from the satellite image (see Fig. 1a).

The simulated variables are compared over 4 special observation sites (Toukamachi, Senjyoji, Shimizu, Naramata) as shown in Figure 1b. On the other hands, observed data using the MU-2 are also selected over 4 domains.

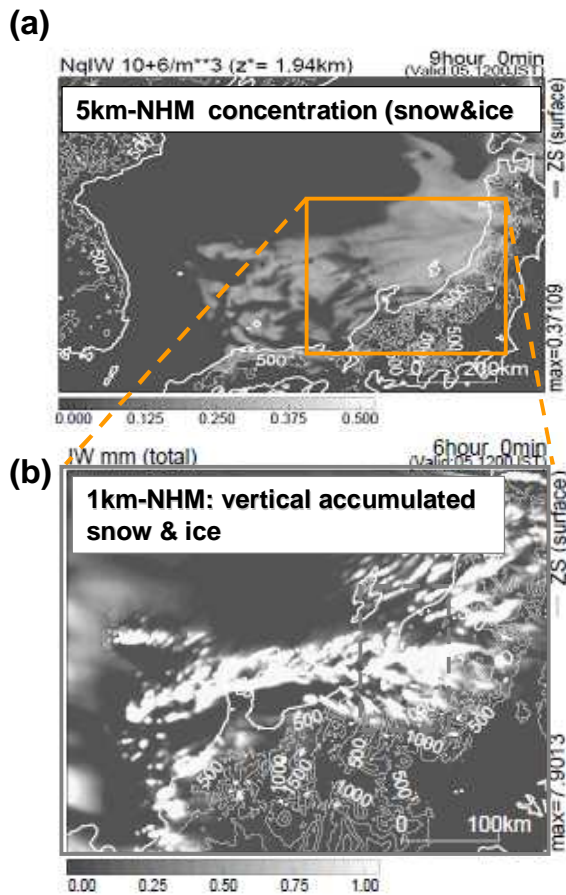


Fig. 2. (a) Concentration of both the snow and ice particles at $z^*=1.94\text{km}$ for simulated by 5km-NHM and (b) vertical accumulation of both snow and ice for simulated by 1km-NHM at the same time. The star in (a) denotes the aircraft observation area.

4. Results

4.1 LWC and IWC

Figure 3a and 3b shows scatter diagram between the simulated and observed LWC in March and December 2007, respectively. Aircraft dataset are took moving average within 10 sec (~ about 1km in

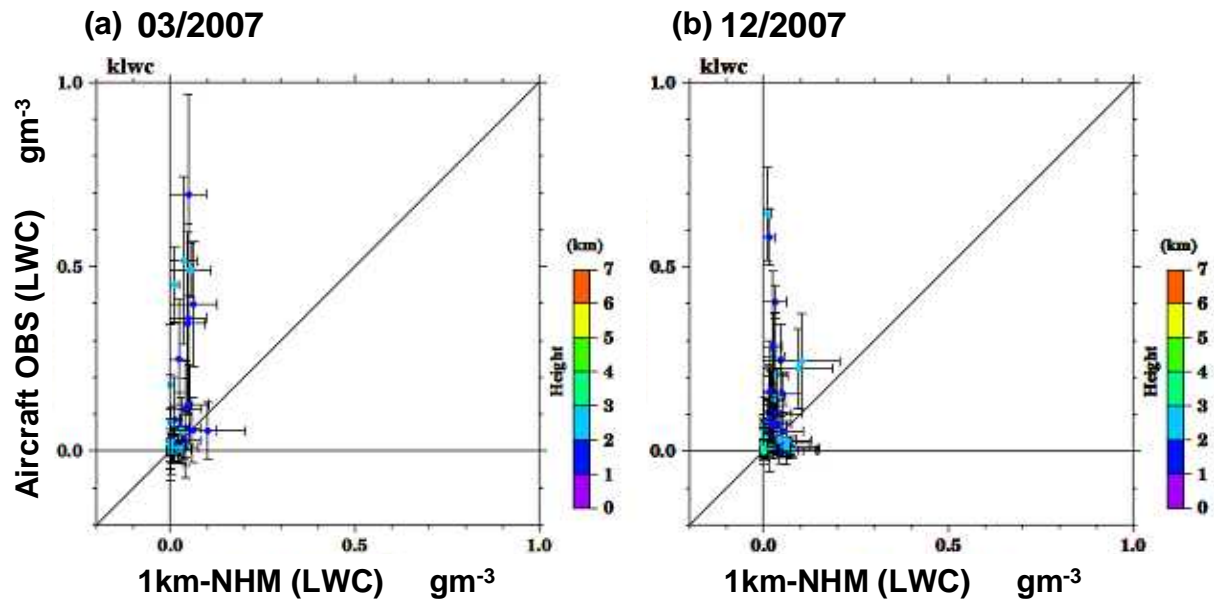


Fig. 3. Scatterplot of LWC simulated by 1km-NHM versus LWC observed by aircraft. Data in March and December 2007 are shown in (a) and (b), respectively. The color scale indicates the heights and the dataset are averaged with heights at every 1km. The standard deviation ($\pm 1\sigma$) for both the observed and simulated LWC are denoted by vertical and horizontal bars, respectively. Observed LWC was measured by the King LWC hot-wire probe.

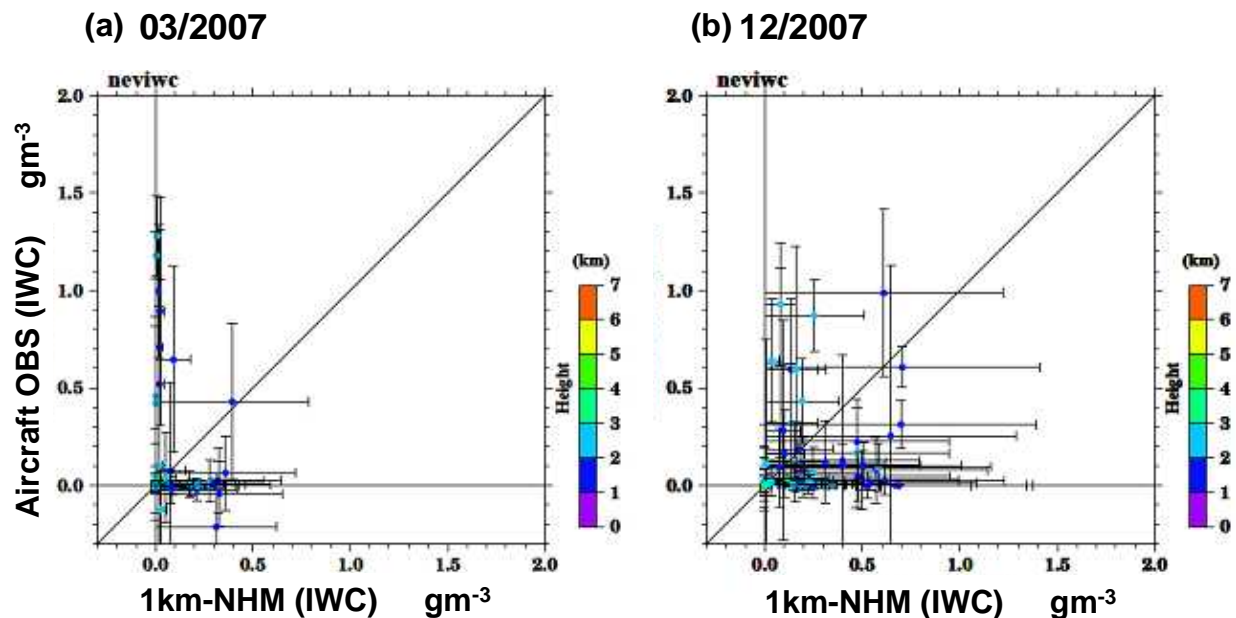


Fig. 4. As in Fig. 3, but for IWC. Observed IWC was defined as $\text{IWC} = \text{Nevzorov TWC} - \text{Nevzorov LWC}$ for March 2007 and $\text{IWC} = \text{Nevzorov TWC} - \text{King LWC}$ for December 2007.

length because aircraft speed is about 100 m/s). The dataset are also averaged with heights at every 1km. Observed LWC was measured by the King LWC hot-wire probe. In March 2007, simulated LWC is underestimated rather than observed LWC. The result in December 2007 is also similar. The dependency of the observational height is unclear. We added error bars which correspond to the standard deviation of each simulated and observed values in Figure 3. The observed error bar is

relatively larger than simulated one.

Figure 4 also shows scatter diagram between the simulated and observed IWC. Observed IWC was calculated by $\text{IWC} = \text{Nevzorov TWC} - \text{Nevzorov LWC}$ in March 2007 and $\text{IWC} = \text{Nevzorov TWC} - \text{King LWC}$ in December 2007. Although these scatter plot is very sporadic, simulated IWC is overestimated rather than observed IWC in some cases. The error bars of the simulated IWC are very large.

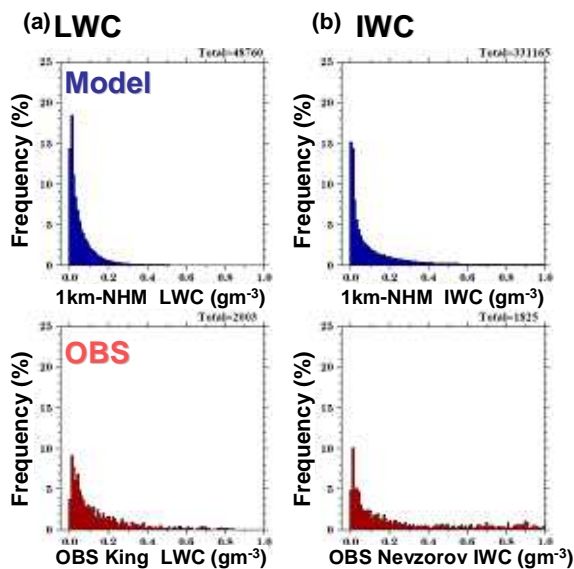


Fig. 5. Frequency distribution of (a) LWC and (b) IWC. The upper panel and downward panels indicate the simulated (blue) and observed by the aircraft (red) LWC and IWC, respectively. The datasets between 1.5 km and 3.0 km in height are shown.

In order to examine the verification of 1km-NHM from the more statistical view point, the frequent appearance of the microphysical properties is investigated. Frequency distributions of LWC and IWC of both the simulation and observation are shown in Fig.5. (a) and (b), respectively. Simulated variables are given at every 6 minutes as described in previous section. These output data are accumulated during 3 hours near the MU-2 observational periods over four special observation

sites. The histogram includes the total flight dataset on December 2007. The datasets between 1.5 km and 3.0 km in height are shown. On the simulated LWC, the frequency of the lower value ($< 0.1 \text{ gm}^{-3}$) is large rather than observed one. On the simulated IWC, the frequency of the lower value ($< 0.1 \text{ gm}^{-3}$) is a little large rather than observed one. On the other hand, the frequency of the relatively higher value ($> 0.4 \text{ gm}^{-3}$) is small while some frequencies of high IWC are found.

These results mean that simulated LWC of 1km-NHM tends to be underestimated, while simulated IWC of that tends to be overestimated in 1km-NHM.

4.2 Concentration of snow

In this subsection, the concentration of snow is also validated between numerical simulation and aircraft observation. Figure 6 shows scatter diagram of snow concentration between the simulated and observed one. The relatively large particle ($> 100 \text{ um}$ in diameter of 2D-C) is defined as snow particles. In both months, simulated concentration of snow is relatively large rather than observed one.

Figure 7 shows frequency distributions of both the simulated and observed snow concentration. Over 3.0 km in height (see Figs. 7c and 7d), the pattern of frequency is very similar. Temperature over 3km in height is under 0 degree in almost cases, so the particles of the precipitation are mainly snow. On the other hand, there are differences between the

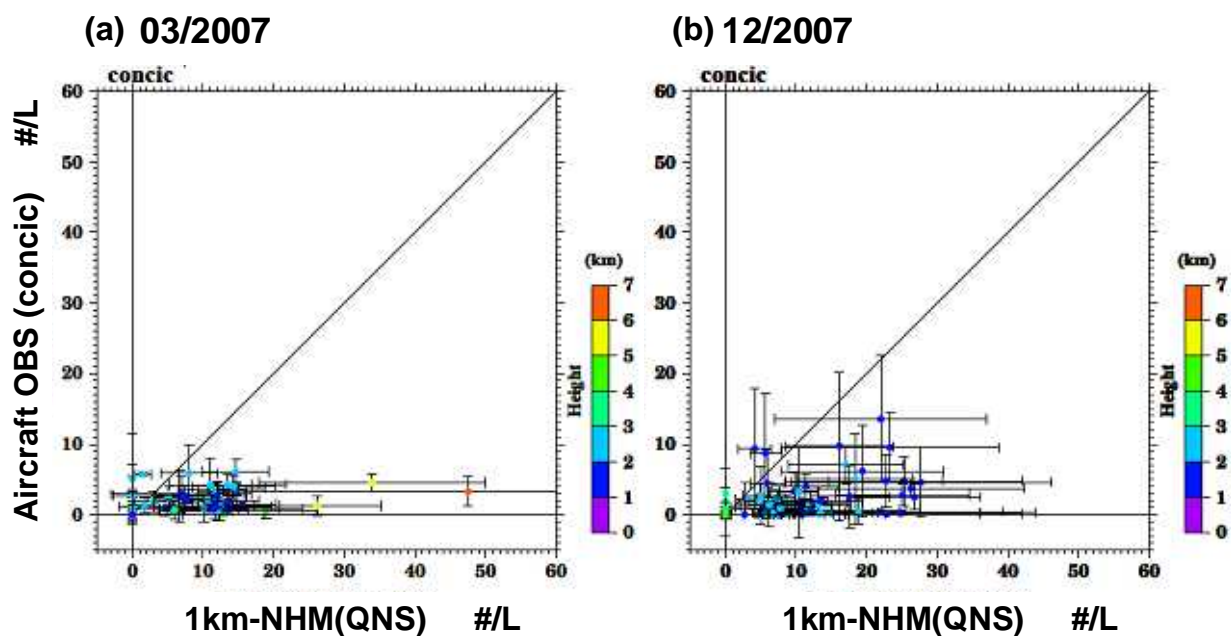


Fig. 6. As in Fig. 3, but for concentration of snow ($> 100 \text{ um}$ in diameter). The data is measured by the two-dimensional cloud (2D-C) probe.

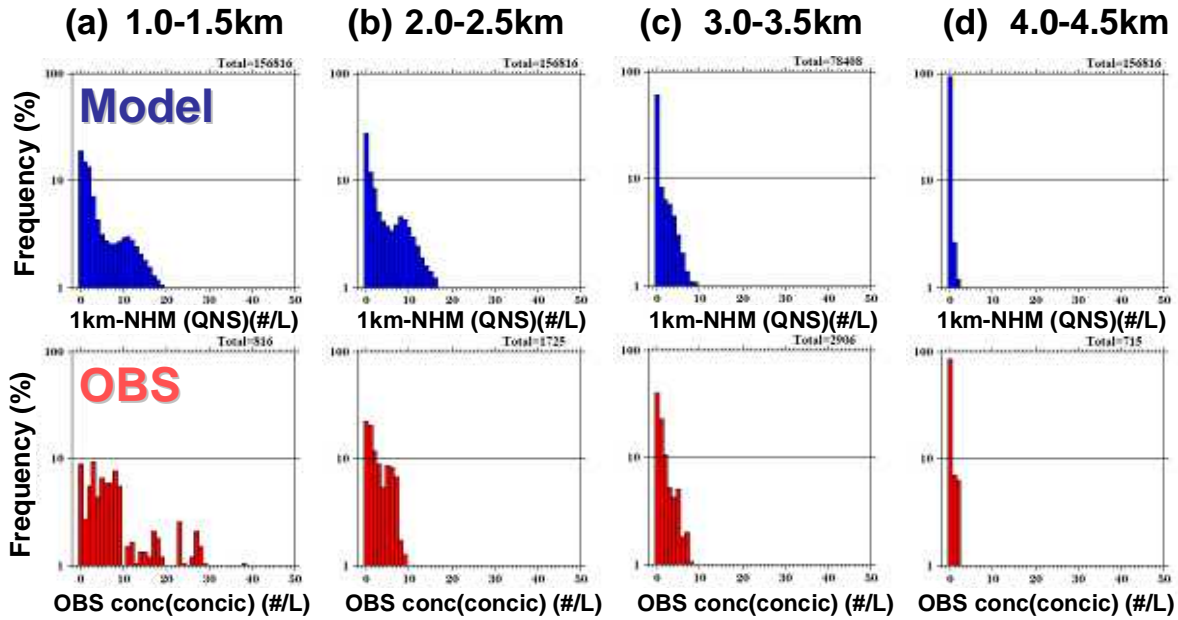


Fig. 7. As in Fig. 5, but for concentration of snow ($> 100 \mu\text{m}$ in diameter). The appearance frequency measured in 1.0-1.5 km, 2.0-2.5 km, 3.0-3.5 km, and 4.0-4.5 km in height are shown in (a), (b), (c), and (d), respectively.

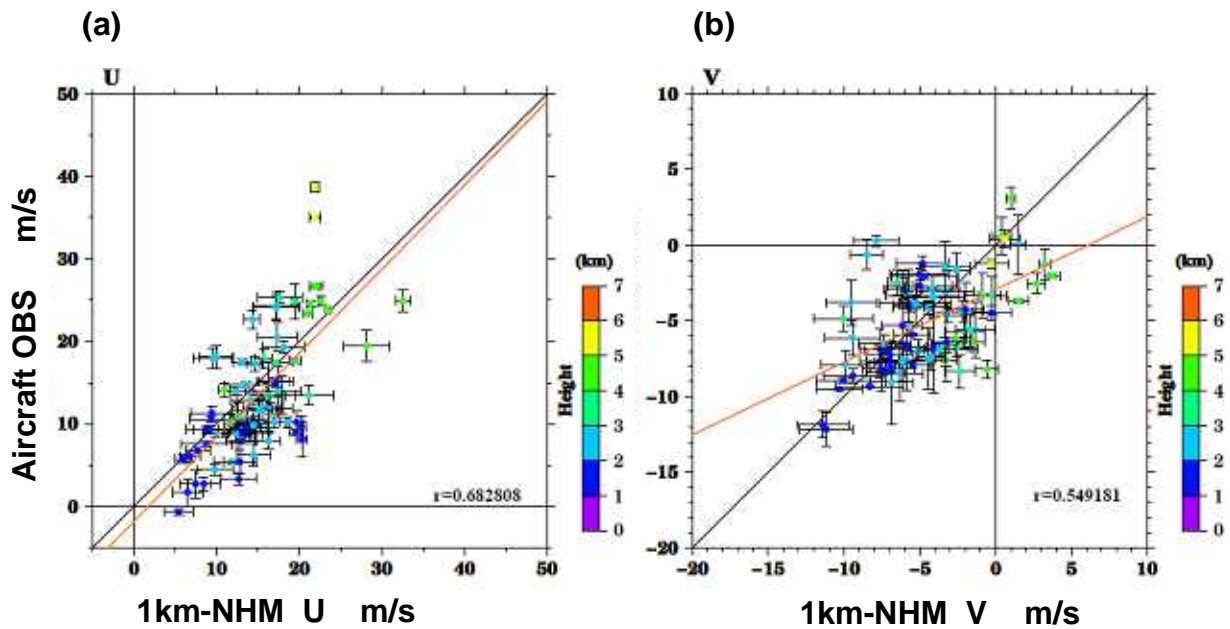


Fig. 8. As in Fig. 3, but for horizontal winds. U and V in December 2007 are shown in (a) and (b), respectively. Solid red line indicates a least squares fitting line.

simulated and observed one in lower height (< 3.0 km in height; see Figs. 7a and 7b). Both the cloud water and ice particles exist in the lower height. The height of the melting layer is variable in the lower layer (surface to 3 km in height around these areas in these winter seasons).

Furthermore, it is difficult to observe by airplane in the lower height because of danger. As a result, there is a little observed data in lower region.

However, the reproducibility of the cloud top

temperature is important for discussing the ice/snow particle concentration. Therefore, the investigation of the cloud top temperature is in progress.

4.3 Wind fields

The dynamical performance of 1km-NHM is also investigated in this subsection. Figure 8 shows scatter diagram of horizontal winds. U and V in December 2007 are shown in (a) and (b) in Fig.8,

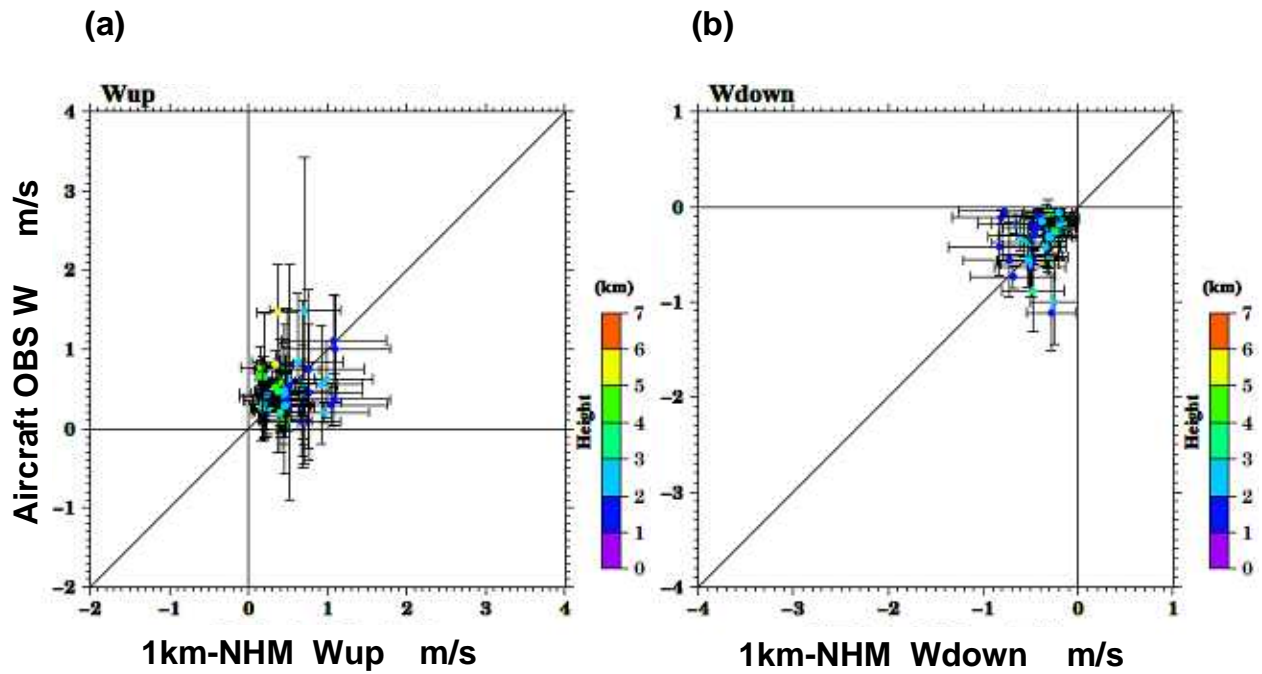


Fig. 9. As in Fig. 3, but for vertical winds. Upward velocity and downward velocity in December 2007 are shown in (a) and (b), respectively.

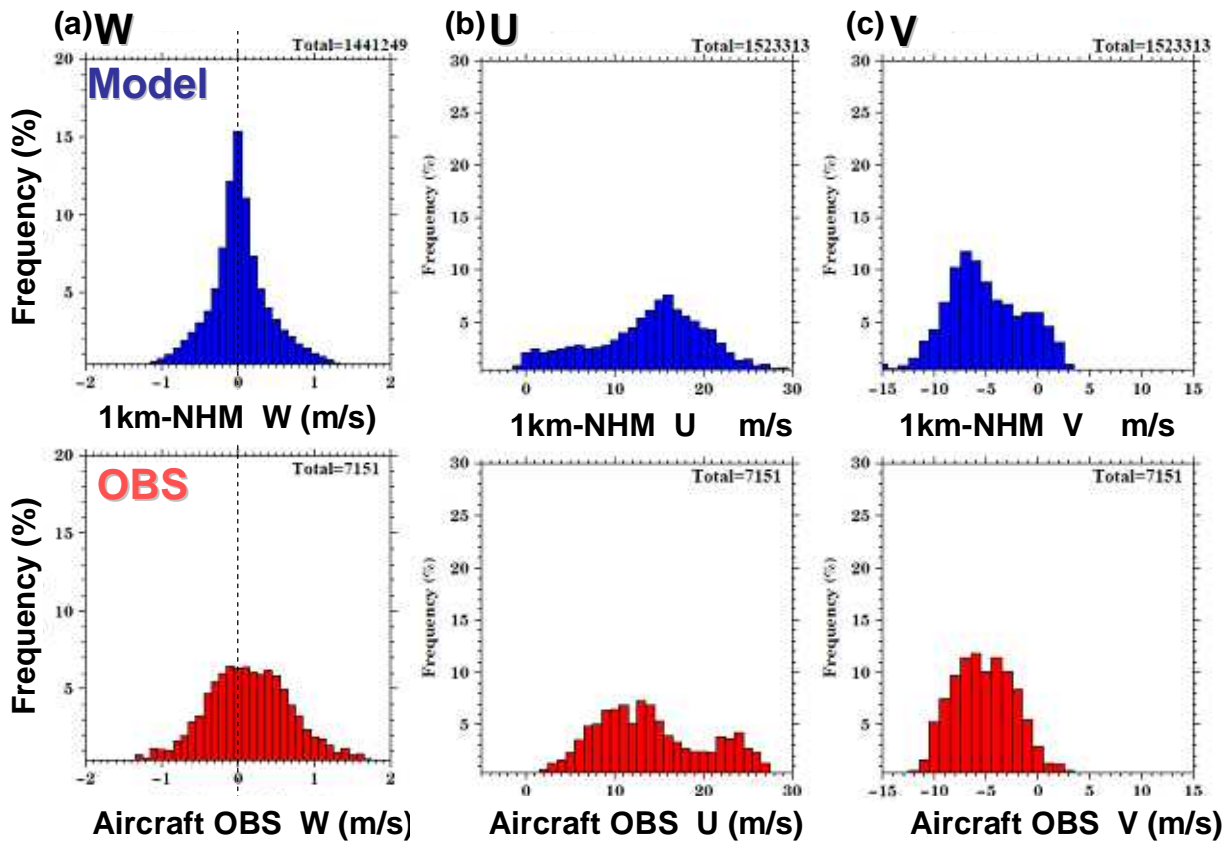


Fig. 10. As in Fig. 5, but for horizontal winds. Vertical velocity (W) and horizontal wind (U and V) are shown in (a), (b), and (c), respectively. The appearance frequency measured 0.0 - 6.0 km in height is shown.

respectively. Both the observed U (V) and simulated U (V) are close to one to one line. These plots are sporadic to some extent because temporal and spatial differences between the observed and

simulated wind speed are large. However, this figure indicates that the simulated horizontal wind fields using a 1km-NHM are reproduced well.

Figure 9 shows scatter diagram of vertical winds.

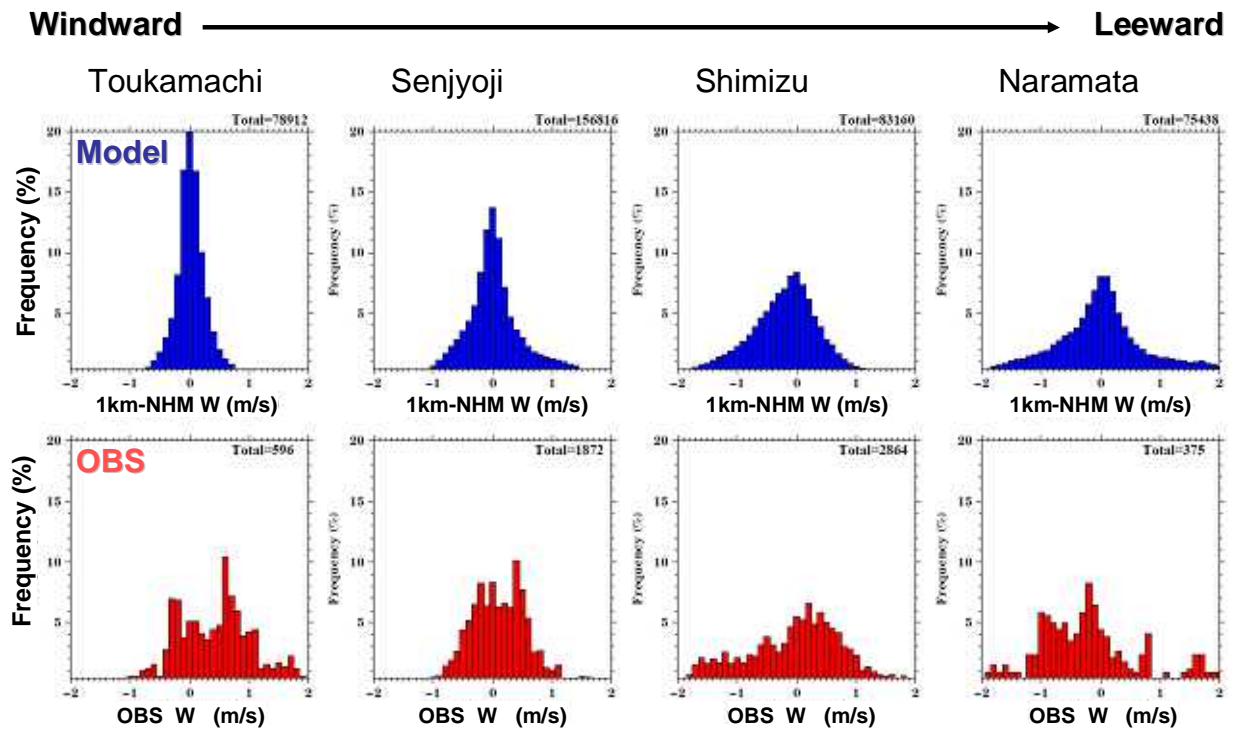


Fig. 11. As in Fig. 5, but for vertical winds at surface special observation sites from windward side (left) to lee side (right). The appearance frequency measured 2.5 - 3.0 km in height is shown.

The upward and downward velocity in December 2007 is shown in (a) and (b) in Fig. 9, respectively. Although these plots are sporadic very well because of the same reason for horizontal wind fields, the order of magnitude for simulated vertical winds agrees with the observed one.

Frequency distributions of vertical velocity (W) and horizontal winds (U and V) are shown in (a), (b), and (c) in Fig. 10, respectively. The data set measured 0.0 - 6.0 km in height is shown. The peak of the model around 0 m/s is relatively large because 1km-NHM can not resolve the realistic topography around Echigo Mountains enough. On the other hand, the frequency of the relatively higher vertical winds ($|w| > 1$ m/s) is smaller rather than that of the observed one. There is no difference of the pattern between the upward and downward winds. However, the pattern of the appearance frequency of the model is agrees with the observed one. The locations of the peak for simulated horizontal wind fields are almost consistent with the observed one (Fig. 10b and 10c).

Figure 11 shows the difference of appearance frequency of vertical wind at every special observation sites. From the windward side to lee side, the amplitude of observed vertical wind speed becomes gradually large because the convection of the snow cloud becomes active due to the effect of the topography around Echigo Mountains. The

patterns for the 1km-NHM simulation are similar to that of observation. The appearance distributions of simulated weaker vertical velocity over the windward special sites (Toukamachi and Senjoji; see Figs. 11a and 11b) are relatively large. It seems that the simulated vertical wind tends to be relatively weak over the windward sides in 1km-NHM. We infer that a horizontal grid spacing of 1km is not enough to resolve the topography of the hilly areas on the windward side.

However, these results means the dynamical properties of 1km-NHM can reproduce the realistic wind fields well, although they include the temporal and spatial differences.

5. Summary

Both of the dynamical and microphysical properties of the cloud resolving model (JMA-NHM) with a horizontal grid spacing of 1 km (1km-NHM) were validated through a series of numerical simulation of the orographic snow clouds cases using in-situ aircraft measurements. The orographic snow clouds in present study were frequently observed in March and December 2007 over the western coastal region of Echigo, center part of Japan. From the view point of the statistical approach, the dynamical and microphysical properties of 1km-NHM was evaluated.

Based on the satellite images, the numerical simulation of 1km-NHM well reproduced the characteristics of the orographic snow clouds.

On the microphysical properties, 1km-NHM tends to underestimate LWC rather than that of our aircraft observation in almost all flights. The simulated IWC is overestimated. The variance is large due to the limits of measurement techniques (Nevzorov IWC) or due to both the temporal and spatial difference between the simulation and observation. Cloud particle concentration of simulated snow is consistent with that of the in-situ observation. The shape of histogram by heights agree with each other in upper layer (~3km). On the other hand, cloud particle concentration of cloud ice and graupel are underestimated (Not shown).

On the dynamical properties, horizontal winds (U and V) are consistent with that of the observed one. That is, simulated wind fields using a 1km-NHM are reproduced well. The order of magnitude for vertical winds (model and observation) agrees with each other. But, the scatter plots of vertical winds are very sporadic (no one to one) because temporal and spatial differences between the model and the observation are large.

The recent previous studies verified the other cloud resolving model using an in situ observation. Colle et al. 2008 simulated the synoptic and mesoscale structures of the event using the Weather Research and Forecasting model (WRF) with horizontal 1.33 km grid spacing during IMPROVE-2 project. They shows that the WRF realistically predicted the ~ 1 m s⁻¹ vertical velocity over the narrow ridges located on the windward (western) face of the Cascades, however it overestimated cloud water production over the ridges.

The dynamical properties of 1km-NHM well reproduced the realistic atmospheric conditions, compared to the previous studies. However, the LWC of 1km-NHM is underestimated too much and the IWC of that is a little overestimated rather than observed one. From the results of the present study, the improvement of the microphysical process of our cloud resolving model is desired to predict LWC and IWC correctly in particular.

Acknowledgments

We express our appreciation to the pilot and ground crew of the research aircraft MU-2 for their support during the observations. We would like to thank Dr. T. Kato of the Japan Meteorological Agency for numerical simulations. This study is supported by the Ministry of Education, Culture,

Sports, Science and Technology of Japan under the program of Special Coordination Funds for Promoting Science and Technology, "Japanese Cloud Seeding Experiments for Precipitation Augmentation (JCSEPA)". The Geostationary Operational Environmental Satellite-9 (GOES-9) visible images were provided by University of Kochi (<http://weather.is.kochi-u.ac.jp/index-e.html>). Generic Mapping Tools (GMT) and Grid Analysis and Display System (GrADS) software were used to draw the figures.

References

- Baumgardner, D., H. Jonsson, W. Dawson, D. O'Connor, and R. Newton (2001), The cloud, aerosol and precipitation spectrometer: A new instrument for cloud investigations, *Atmos. Res.*, 59–60, 251–264, doi:10.1016/S0169-8095(01)00119-3.
- Colle, B. A., J. B. Wolfe, W. J. Steenburgh, D. E. Kingsmill, J. A. W. Cox, and J. C. Shafer, 2005: High-resolution simulations and microphysical validation of an orographic precipitation event over the Wasatch Mountains during IPEX IOP3. *Mon. Wea. Rev.*, **133**, 2947–2971.
- Colle, B. A., Y. Lin, S. Medina, and B. F. Smull, 2008: Orographic Modification of Convection and Flow Kinematics by the Oregon Coast Range and Cascades during IMPROVE-2. *Mon. Wea. Rev.*, **136**, 3894–3916.
- Garvert, M. F., B. A. Colle, and C. F. Mass, 2005: The 13–14 December 2001 IMPROVE-2 event. Part I: Synoptic and mesoscale evolution and comparison with a mesoscale model simulation. *J. Atmos. Sci.*, **62**, 3474–3492.
- Garvert, M. F., C. P. Woods, B. A. Colle, C. F. Mass, P. V. Hobbs, M. T. Stoelinga, and J. B. Wolfe (2005), The 13-14 December 2001 IMPROVE-2 event. Part II: Comparison of MM5 model simulations of clouds and precipitation with observations, *J. Atmos. Sci.*, **62**, 3520–3534.
- Gerber, H., B. G. Arends, and A. S. Ackerman, 1994: New microphysics sensor for aircraft use. *Atmos. Res.*, **31**, 235–252.
- Guan, H., S. G. Cober, and G. A. Isaac (2001), Verification of supercooled cloud water forecasts with in situ aircraft measurements, *Weather Forecasting*, **16**, 145–155.

- Guan, H., S. G. Cober, G. A. Isaac, A. Tremblay, and A. Me'thot (2002), Comparison of three cloud forecast schemes with in situ aircraft measurements, *Weather Forecasting*, **17**, 1226–1235.
- Hashimoto, A., T. Kato, S. Hayashi, and M. Murakami, 2008: Seedability assessment for winter orographic snow clouds over the Echigo Mountains, *SOLA*, **4**, 069-072.
- Kato, T., A. Hashimoto, and S. Hayashi, 2008: A Numerical Study on the Appearance of Target Clouds for Artificial Precipitation Experiments over Shikoku Island, Western Japan during the Baiu Season. *SOLA*, **4**, 081-084.
- King, W. D., D. A. Parkin, and R. J. Handsworth (1978), A hot-wire water device having fully calculable response characteristics, *J. Appl. Meteorol.*, **17**, 1809–1813.
- Knollenberg, R. G. (1981), Techniques for probing cloud microstructure, in *Clouds, Their Formation, Optical Properties, and Effects*, edited by P. V. Hobbs and A. Deepak, pp. 15–89, Academic, New York.
- Korolev, A. V., J. W. Strapp, G. A. Isaac, and A. N. Nevzorov, 1998: The Nevzorov airborne hot-wire LWC-TWC probe: Principle of operation and performance characteristics, *J. Atmos. Oceanic Technol.*, **15**, 1495–1510.
- Luo, Y., K-M. Xu, H. Morrison, and G. McFarquhar, 2008): Arctic mixed phase clouds simulated by a cloud-resolving model: Comparison with ARM observations and sensitivity to microphysics parameterizations, *J. Atmos. Sci.*, **65**, 1285–1303, doi:10.1175/2007JAS2467.1.
- Luo, Y., K-M. Xu, H. Morrison, and G. McFarquhar, 2008: Arctic Mixed-Phase Clouds Simulated by a Cloud-Resolving Model: Comparison with ARM Observations and Sensitivity to Microphysics Parameterizations. *J. Atmos. Sci.*, **65**, 1285-1303.
- Mavromatidis, E. and Kallos, G., 2003: An investigation of cold cloud formation with a three-dimensional model with explicit microphysics. *J. Geophys. Res.*, **108**, NO. D14, 4420, doi:10.1029/2002JD002711.
- Milbrandt, J. A., M. K. Yau, J. Mailhot, and S. B. éclair, 2008: Simulation of an Orographic Precipitation Event during IMPROVE-2. Part I: Evaluation of the Control Run Using a Triple-Moment Bulk Microphysics Scheme. *Mon. Wea. Rev.*, **136**, 3873–3893.
- Morrison, H., J. O. Pinto, J. A. Curry, and G. M. McFarquhar (2008), Sensitivity of modeled arctic mixed-phase stratocumulus to cloud condensation and ice nuclei over regionally varying surface conditions, *J. Geophys. Res.*, **113**, D05203, doi:10.1029/2007JD008729.
- Saito, K., T. Fujita, Y. Yamada, J. Ishida, Y. Kumagai, K. Aranami, S. Ohmori, R. Nagasawa, S. Kumagai, C. Muroi, T. Kato, H. Eito, Y. Yamazaki, 2006: The operational JMA nonhydrostatic mesoscale model. *Mon. Wea. Rev.*, **134**, 1266–1298.
- Strapp, J. W., J. Oldenburg, R. Ide, L. Lilie, S. Bacic, Z. Vukovic, M. Oleskiw, D. Miller, E. Emery, and G. Leone (2003), Wind tunnel measurements of the response of hot-wire liquid water content instruments to large droplets, *J. Atmos. Oceanic Technol.*, **20**, 791–806.
- Vaillancourt, P. A., A. Tremblay, S. G. Cober, and G. A. Isaac (2003), Comparison of aircraft observations with mixed-phase cloud simulations, *Mon. Wea. Rev.*, **131**, 656–671.
- Zhang, J., W. Gong, W. R. Leitch, and J. W. Strapp, 2007: Evaluation of modeled cloud properties against aircraft observations for air quality applications. *J. Geophys. Res.*, **112**, D10S16, doi:10.1029/2006JD007596.
- Yoshida, Y., M. Murakami, Y. Kurumizawa, T. Kato, A. Hashimoto, T. Yamazaki, and N. Haneda, 2009: Evaluation of snow augmentation by cloud seeding for drought mitigation. *J. Japan. Soc. Hydrol. and Water Resour.*, **22**, 209-222.